0026-895X/08/7405-1443–1452$20.00
MOLECULAR PHARMACOLOGY
Vol. 74, No. 5
49056/3397575
Mol Pharmacol 74:1443–1452, 2008
Printed in U.S.A.

Drug Binding to the Inactivated State Is Necessary but Not Sufficient for High-Affinity Binding to Human *Ether-à-go-go*-Related Gene Channels[S]

Mark J. Perrin, Philip W. Kuchel, Terence J. Campbell, and Jamie I. Vandenberg

Mark Cowley Lidwill Research Program in Electrophysiology and Biophysics, Victor Chang Cardiac Research Institute, New South Wales, Australia (M.J.P., T.J.C., J.I.V.); St. Vincent's Clinical School, University of New South Wales, New South Wales, Australia (M.J.P., T.J.C., J.I.V.); and School of Molecular and Microbial Biosciences, University of Sydney, New South Wales, Australia (P.W.K., J.I.V.)

Received May 21, 2008; accepted August 13, 2008

ABSTRACT

Drug block of the human *ether-à-go-go*-related gene K^+ channel (hERG) is the most common cause of acquired long QT syndrome, a disorder of cardiac repolarization that may result in ventricular tachycardia and sudden cardiac death. We investigated the open versus inactivated state dependence of drug block by using hERG mutants N588K and N588E, which shift the voltage dependence of inactivation compared with wild-type but in which the mutated residue is remote from the drug-binding pocket in the channel pore. Four high-affinity drugs (cisapride, dofetilide, terfenadine, and astemizole) demonstrated lower affinity for the inactivation-deficient N588K mutant hERG channel compared with N588E and wild-type hERG. Three of four low-affinity drugs (erythromycin, perhexiline, and quinidine) demonstrated no preference for N588E over N588K channels, whereas *dl*-sotalol was an example of a low-affinity state-dependent blocker. All five state-dependent blockers showed an even lower affinity for S620T mutant hERG (no inactivation) compared with N588K mutant hERG (greatly reduced inactivation). Computer modeling indicates that the reduced affinity for S620T compared with N588K and wild-type channels can be explained by the relative kinetics of drug block and unblock compared with the kinetics of inactivation and recovery from inactivation. We were also able to calculate, for the first time, the relative affinities for the inactivated versus the open state, which for the drugs tested here ranged from 4- to 70-fold. Our results show that preferential binding to the inactivated state is necessary but not sufficient for high-affinity binding to hERG channels.

The human *ether-à-go-go*-related gene (hERG) encodes the pore-forming subunit of the ion channel that conducts the rapid component of the delayed rectifier potassium current (I_{Kr}) in the heart (Sanguinetti et al., 1995). Gain and loss of function mutations in hERG may result in the clinical conditions of short QT syndrome (SQTS) (Brugada et al., 2004) and long QT syndrome (Curran et al., 1995), respectively, underscoring the crucial role of hERG in maintaining electrical stability in the heart. The congenital form of long QT syndrome is uncommon and may result from mutations in 10 different genes, most encoding ion channels or their regulatory subunits (Roden, 2008). Acquired long QT syndrome, through drug-induced blockade of hERG, is more frequent (Sanguinetti et al., 1995; Roden, 2004) and is a common reason for the withdrawal of medications from the pharmaceutical market (Roden, 2004). As a result, early assessment of a drug's affinity for hERG has been mandated (Guth, 2007) and obliges the need for a detailed understanding of how drugs bind to hERG.

It is well established that drugs bind in the central cavity of the pore region of hERG (Mitcheson et al., 2000) and that channels need to open before this can occur (Kiehn et al., 1996). At depolarizing potentials, hERG channels can exist in either an open or an inactivated state (Sanguinetti et al., 1995; Smith et al., 1996), yet is has not been established whether the open or the inactivated state is preferred for drug binding. Evidence in support of preferential binding to the inactivated state comes primarily from studies showing reduced affinity for mutant channels that either abolish (S620T; G628C + S631C) or reduce inactivation (S631A)

This work was supported in part by project grants from the St. Vincent's Clinic Foundation (to T.J.C.) and a Widdifield Cardiac Research Scholarship (to M.J.P.). J.I.V. is a National Health and Medical Research Council Senior Research Fellow.
Article, publication date, and citation information can be found at http://molpharm.aspetjournals.org.
doi:10.1124/mol.108.049056.
[S] The online version of this article (available at http://molpharm.aspetjournals.org) contains supplemental material.

ABBREVIATIONS: hERG, human *ether-à-go-go*-related gene; SQTS, short QT syndrome; WT, wild type; CHO, Chinese hamster ovary cell; DMSO dimethyl sulfoxide; E-4031, 2-methyl-6-(2-(4-(4-methylsulfonylamino)benzoylpiperidin-1-yl)ethyl)pyridine.

(Ficker et al., 1998; Weerapura et al., 2002). These mutations, however, lie proximate to the selectivity filter and putative drug-binding pocket (Fig. 1) and so may affect drug block by gating-independent means through local changes in the drug-binding pocket. To address this concern, we investigated whether mutations to residues that are remote from the central pore but affect inactivation would also alter drug binding to hERG in a manner similar to that reported for the S631A and S620T mutants. Specifically, we mutated residue Asn588, located on the α-helix of the S5P linker (Torres et al., 2003) and believed to be distant from the drug-binding pocket (Yi et al., 2007), to either glutamate (N588E) or lysine (N588K) (Clarke et al., 2006).

In this study we characterized the binding of four high-affinity blockers (dofetilide, cisapride, astemizole, and terfenadine) and four low-affinity blockers (quinidine, perhexiline, erythromycin, and *dl*-sotalol). All four high-affinity blockers exhibited reduced affinity for the inactivation-deficient mutants (N588K and S620T), whereas only *dl*-sotalol among the low-affinity blockers showed reduced affinity for N588K. In all cases in which binding was affected by inactivation-deficient mutants, the affinity for S620T was markedly lower than for N588K mutant channels. A kinetic model of drug binding indicated that the difference between drug binding to wild-type (WT), N588K, and S620T channels can be explained by the kinetics of drug block with the affinity for the open state being reduced 4- to 70-fold compared with the inactivated state, depending on the particular drug studied.

Our results show that preferential binding to the inactivated state is necessary but not sufficient for high-affinity binding to hERG channels. Furthermore, we propose that the affinity of drugs for the S620T mutant represents their true affinity for the open conformation of the channel, and the measured affinity for the WT channel is a weighted average of the affinity for the open and inactivated states. Furthermore, for the first time, we have provided quantitative assessments of the relative affinities of different drugs for the open and inactivated states of hERG.

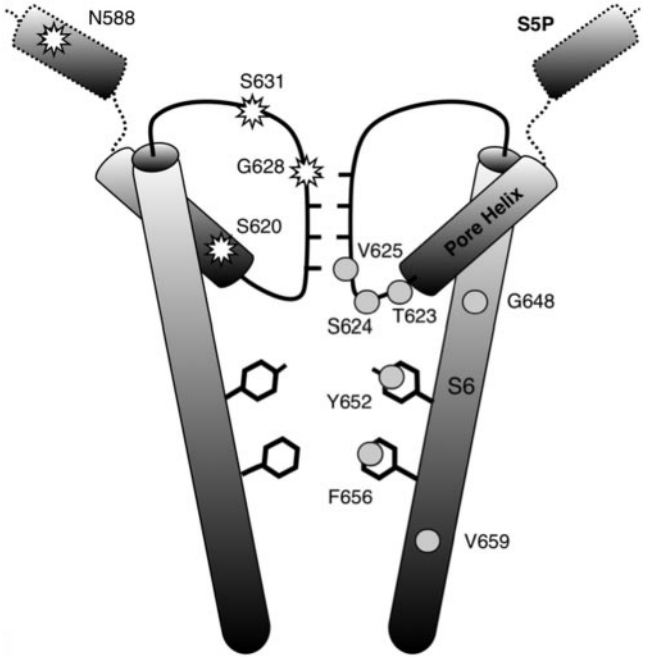

Fig. 1. Schematic diagram of the Ser5, Ser6, pore helix, and S5P linker regions of two hERG subunits. The most important molecular determinants of drug block are denoted with gray circles. Commonly used mutants that disrupt inactivation are displayed with white stars. Note that Gly648 is probably not exposed to the pore cavity and is believed to influence drug block by determining the conformation of the drug binding pocket; Val659 may influence drug block by altering the gating characteristics of the channel (Mitcheson et al., 2000; Mitcheson, 2008). The S5P linker is broken, because its exact position relative to the pore is unknown.

Materials and Methods

Molecular Biology

Experiments on WT hERG channels were performed using a Chinese hamster ovary (CHO) cell line stably expressing the hERG K^+ channel (hERG cDNA kindly donated by Dr. Gail Robertson) constructed as described previously (Walker et al., 1999b). CHO cells were cultured in Dulbecco's modified Eagle's medium/F-12 with 10% fetal bovine serum and maintained at 37°C in 5% CO_2. Cells were studied at least 24 h after being plated on microscope coverslips. Mutant hERG constructs were generated using the Megaprimer polymerase chain reaction method (Clarke et al., 2006). Mutant constructs (N588K, N588E, S631A, or S620T) were sequenced to ensure that only the correct mutation had been made and then were subcloned into the pIRES2-enhanced green fluorescent protein vector. Blank CHO cells were plated onto sterilized glass coverslips. After 24 h, the cells were transfected with mutant hERG constructs using PolyFect Transfection Reagent (QIAGEN, Valencia, CA) according to the manufacturer's instructions. After transfection, the cells were incubated at 37°C for a minimum of 1 day before electrophysiological study. Successfully transfected cells, identified by the expression of enhanced green fluorescent protein, were studied using the whole-cell configuration of the patch-clamp technique.

Electrophysiology

Borosilicate glass tubing patch pipettes, with resistances of 1 to 4 MΩ when filled with internal solution, were made using a vertical two-stage puller (PP-830; Narishige, Tokyo, Japan). The internal solution contained 120 mM potassium gluconate, 20 mM KCl, 1.5 mM MgATP, 5 mM EGTA, and 10 mM HEPES, pH 7.3 with KOH. Membrane potentials were adjusted by −15 mV to correct for the junction potential (calculated using the JPcalc algorithm in pClamp 9; Molecular Devices, Sunnyvale, CA) between low Cl^- pipette solution and external bath solution (see below). Currents were amplified (Axopatch 200B amplifier; Molecular Devices) and digitized (Digi-Data 1200; Molecular Devices) before storage on a personal computer. Capacitance current transients were electronically subtracted, and series resistance compensation was ~80% for all experiments. Current signals were digitized at 5 kHz and low-pass-filtered at 2 kHz. Some current traces were leak-subtracted offline. Acquisition was performed using pClamp software.

Solutions and Drugs

Cells were superfused with a Tyrode's solution containing 130 mM NaCl, 5 mM KCl, 1 mM MgCl, 1 mM $CaCl_2$, 12.5 mM glucose, and 10 mM HEPES. *dl*-Sotalol was purchased from Bristol-Myers Squibb (Victoria, Australia). All other drugs were purchased from Sigma-Aldrich (New South Wales, Australia). Cisapride, astemizole, terfenadine, erythromycin, dofetilide, and quinidine were prepared as stock solutions in dimethyl sulfoxide (DMSO) and subsequently diluted as required with superfusate [maximum final DMSO concentration, 0.1% (v/v)]. *dl*-Sotalol was prepared as a stock solution in Tyrode's solution and perhexiline as a stock solution in methanol. We have reported previously that DMSO at 0.1% (v/v) has no effect on the parameters under study (Walker et al., 1999b).

Voltage Protocols

Steady-State Inactivation. From a holding potential of −80 mV, the membrane voltage was stepped to +40 mV for 3 s to fully activate the channels. For cells expressing WT-hERG and N588E-hERG, the second pulse consisted of a voltage step from +40 mV to −160 mV in 10-mV decrements. For cells expressing N588K, a range of +120 to −20 mV was used . For voltage steps to < −30 mV, an exponential curve was fitted to the first phase of deactivation and extrapolated back to the beginning of the second pulse, at which point its magnitude represents the current that the channel would have passed if recovery from inactivation were instantaneous. Channel conductance was plotted against voltage to yield the voltage-dependent steady-state inactivation curve (properly, the steady-state recovery from inactivation), and the data were fitted with a Boltzmann function:

$$\frac{G}{G_{max}} = \frac{1}{(1 + e^{(V_{0.5} - V_t)/k})}$$

where $V_{0.5}$ represents half-inactivation voltage, and k is the slope factor.

Drug Block. Because this was a comparative study, care was taken to ensure similar conditions for drug testing in WT and mutant channels. However, because of the unique gating characteristics of N588E-hERG and N588K-hERG, slight alterations in the voltage protocol and method of measurement were used. Currents were measured with a two-step voltage protocol: a first step to +20 mV for 3 s to fully activate the channels, and a second step to a negative membrane potential, usually −110 mV (but see below for variations). During this second voltage step, hERG channels quickly recover from inactivation and proceed to deactivate. This second step was termed "revelatory" because it allowed us to estimate the total conductance of activated channels (open and inactivated) after the 3-s period of depolarization.

The revelatory step was typically recorded at −110 mV, although in some N588E-hERG cells, a voltage step to −120 mV was used to allow adequate recovery from inactivation for current measurement. On the other hand, a less negative voltage was used for a few N588K-hERG cells to minimize series resistance errors due to the large activating current in this nonrectifying construct. Drug block was calculated as $I_{[drug]}/I_{control}$, with all currents measured at the end of the activating step. For N588E-hERG and WT-hERG, a single exponential fit was applied to the first part of the current trace during the revelatory step and extrapolated back to the end of the activating step. In this way, current was measured at the same time point for all cells.

Voltage-protocols were repeated at 0.1 Hz. Control currents were recorded 3 to 5 min after patch rupture (i.e., the time take for current levels to stabilize at a steady-state level). The first drug was applied, with solution exchange typically taking less than 10 s. Recording continued until a new steady-state block was reached (typically 2–4 min). Between two and four doses of drug were applied to each cell, with most experiments completed within 20 min.

Data Analysis

Initial data analysis was performed using the Clampfit module of the pClamp 9.0 software. Subsequent data analysis and preparation of data for figures were performed with Mathematica 6 (Wolfram Technologies, Champaign, IL). All data are expressed as mean ± S.E.M. (n), and statistical significance ($P < 0.05$) was determined using paired t tests.

Results

$V_{0.5}$ of Steady-State Inactivation in WT-hERG, N588E-hERG, and N588K hERG Expressed in CHO Cells. To investigate the link between drug binding and state dependence, we chose to use mutants of residue Asn588 located in the α-helix of the S5P linker of hERG (Fig. 1). This residue has two important features: first, it is believed to be located distant to the drug binding pocket (Yi et al., 2007); and second, it is possible to titrate the voltage dependence of inactivation of the channels by introducing different charges at this residue (Clarke et al., 2006).

Our previous studies of Asn588 mutant channels were carried out using the *Xenopus laevis* oocyte expression system; however, mammalian cells are the preferred heterologous expression system to use for drug binding studies (Cavalli et al., 2002). Therefore, we first wanted to confirm that the properties of Asn588 mutant channels were similar in mammalian cells and *X. laevis* oocytes. When expressed in CHO cells, the $V_{0.5}$ of inactivation for N588E-hERG was −114 ± 3 mV with a slope factor of −19 ± 1 mV (n = 13); the $V_{0.5}$ of inactivation for WT-hERG was −78 ± 2 mV with a slope factor of −27 ± 2 mV (n = 11); and the $V_{0.5}$ of inactivation for N588K-hERG was 45 ± 4 mV with a slope factor of −14 ± 1 mV (n = 6) (Fig. 2). All values are similar to those reported for *X. laevis* oocytes (Clarke et al., 2006). The reversal potential for N588K-hERG, − 83.4 ± 2.0 mV (n = 5), was slightly shifted compared with that for WT-hERG, − 88.5 ± 2.2 mV (n = 10). This is very similar to previous reports (Cordeiro et al., 2005). The N588K-hERG channels are nevertheless still highly selective for K^+ over Na^+. The reversal potential in the N588E-hERG construct could not be determined because of the small magnitude of its activating currents. However, when expressed in oocytes with much larger currents, it was found to be similar to WT-hERG (Clarke et al., 2006). These properties together make Asn588 mutant constructs ideal for the investigation of inactivation mediated drug-binding to hERG.

High-Affinity Drug Binding Is Modulated by Asn588 Charge Mutants. We initially investigated the affinity of four drugs, established previously to block hERG in the low nanomolar range—astemizole (Zhou et al., 1999), cisapride (Mohammad et al., 1997), dofetilide (Kiehn et al., 1996), and terfenadine (Yang et al., 2004)—for N588E-hERG, WT-hERG, and N588K-hERG expressed in CHO cells. Figure 3 shows typical examples of WT-, N588E-, and N588K-hERG traces under control conditions and after 5-min equilibration with 30 nM cisapride. Percentage of drug block was mea-

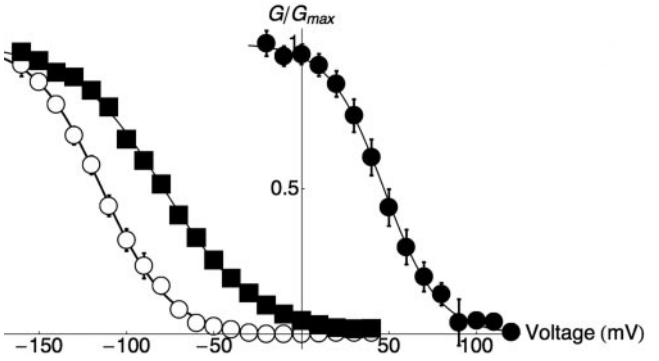

Fig. 2. Conductance voltage curves for N588E-hERG (○), WT-hERG (■), and N588K-hERG (●). Data points are mean ± S.E.M., and the curve fitted to the data is a Boltzmann function with a $V_{0.5}$ of inactivation of −114 ± 3 mV and slope factor of −19 mV (n = 13) for N588E-hERG, $V_{0.5}$ of −78 ± 2 mV and slope factor of −26 mV (n = 11) for WT-hERG, and a $V_{0.5}$ of 45 ± 4 mV and slope factor of −14 mV (n = 6) for N588K-hERG.

sured at the end of the 3-s activating step to +20 mV in all cells. This was performed directly in N588K (Fig. 3C) or else by fitting a single exponential curve to the first part of the current trace during the revelatory step in N588E-hERG (Fig. 3B) and WT-hERG (Fig. 3A) and extrapolating this back to the end of the activating step. The data in Fig. 3 indicate that 30 nM cisapride caused less block of N588K-hERG channels compared with N588E- or WT-hERG. This is more clearly seen from the summary Hill plots shown in Fig. 4; cisapride affinity for WT-hERG, 20.5 ± 2.2 nM (n = 4), was similar to that for N588E-hERG, 13.1 ± 4.9 nM (n = 4), but significantly reduced for N588K-hERG, 55.9 ± 4.2 nM (n =

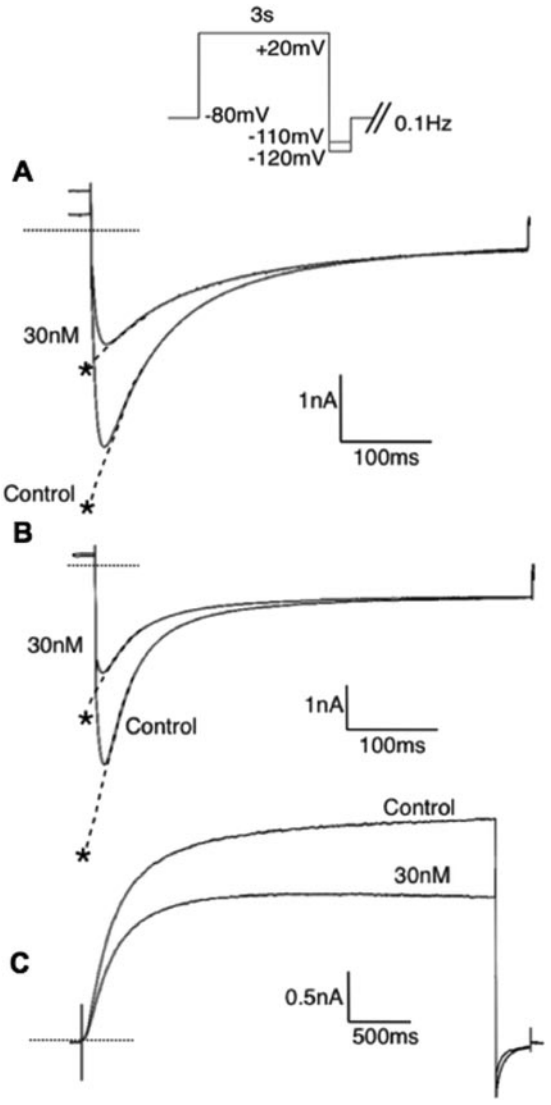

Fig. 3. Typical examples of current traces recorded from the drug-block voltage protocol illustrated at top. WT-hERG (A) N588E-hERG (B), and N588K-hERG (C) in the presence of 30 nM cisapride. Broken lines represent zero current in each case. Note the different scales on each recording; A and B show currents recorded during the revelatory voltage step, whereas C displays the nonrectifying current of the 3-s depolarizing step in N588K-hERG. The percentage of drug block for each recording was determined by dividing the current measured at the end of the 3-s depolarizing step to +20 mV after application of the drug (I_{drug}) by the current measured at the beginning of the recording ($I_{control}$). In the case of WT-hERG and N588E-hERG, the current at this point was determined by fitting an exponential curve to the first part of the deactivating current during the revelatory voltage step and extrapolating this back to the end of the depolarizing step, as illustrated in A and B.

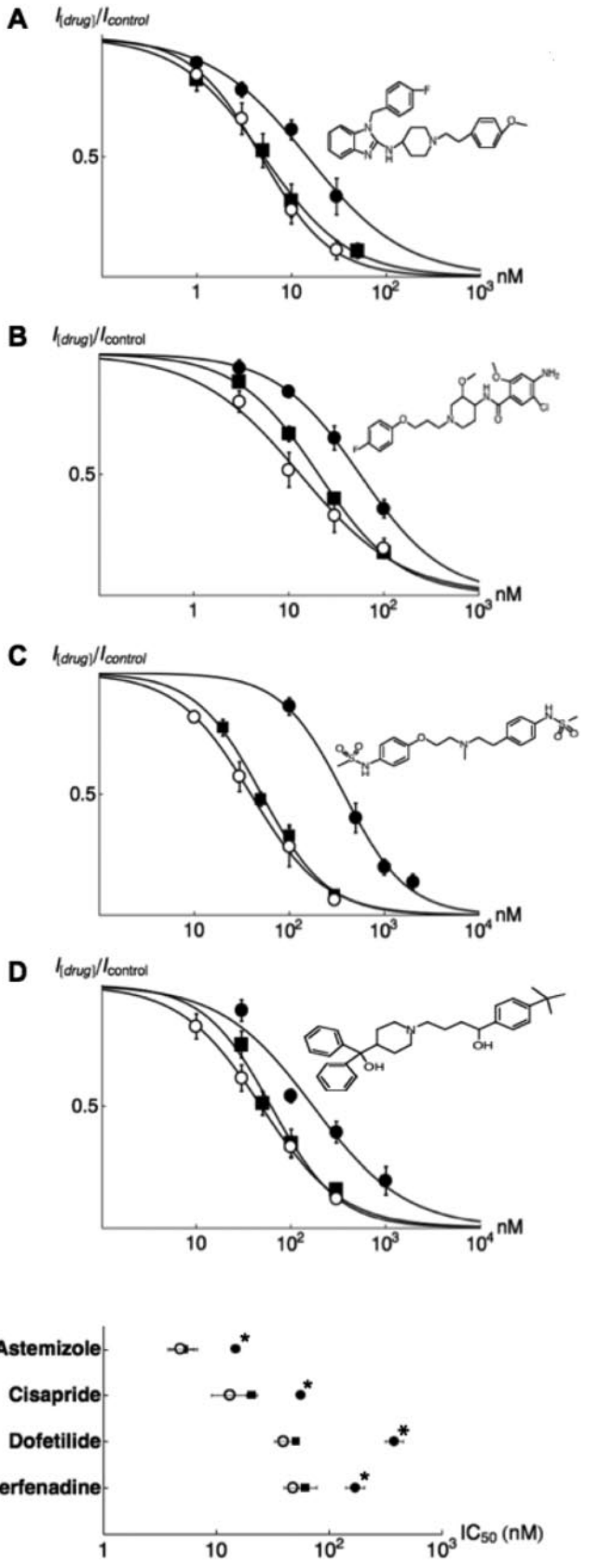

Fig. 4. Hill plots of high-affinity hERG blockers. Drug-binding to WT-hERG (■), N588E-hERG (○), and N588K-hERG (●) for astemizole (A) cisapride (B), dofetilide (C), and terfenadine (D). Each data point represents $I_{[drug]}/I_{control}$ ± S.E.M. for n = 4 to 9 cells. E, summary data showing the mean IC_{50} ± S.E.M. for each drug. Significant differences between WT-hERG and N588K-hERG are denoted by ∗. All values are listed in Table 1.

4). All four high-affinity blockers showed a similar pattern of reduced affinity for N588K- compared with WT- and N588E-hERG (see Fig. 4). The affinities for all drugs for WT and Asn588 mutant constructs are summarized in Table 1.

Low-Affinity Drug Binding to Asn588 Charge Mutants. We next investigated the affinity of four drugs established previously to block hERG in the high nanomolar or micromolar range—quinidine (Lees-Miller et al., 2000), perhexiline (Walker et al., 1999a), erythromycin (Volberg et al., 2002), and *dl*-sotalol (Kirsch et al., 2004)—for N588E-hERG, WT-hERG, and N588K-hERG constructs expressed in CHO cells. Typical examples of current traces recorded from WT-, N588K-, and N588E-hERG in the presence and absence of 3 μM quinidine are illustrated in Fig. 5. Quinidine caused a similar degree of block of WT and the two Asn588 charge mutants. This is also seen from the summary Hill plots (Fig. 6A). Perhexiline and erythromycin showed the same pattern as that observed for quinidine (i.e., similar affinities for all hERG constructs) (Fig. 6, A and C). In contrast, *dl*-sotalol showed a significantly higher affinity for N588E-hERG and WT-hERG compared with N588K-hERG (Fig. 6D and Table 1).

Does Reduced Affinity for N588K-hERG Reflect State-Dependent Binding? The data from Figs. 3 and 4 clearly demonstrate that the four high-affinity drugs used in this study had reduced affinity for the inactivation-deficient N588K-hERG channels. To determine whether this reduced affinity for N588K-hERG reflected a state dependence of drug binding, we investigated whether there was a similarly reduced affinity for a range of inactivation-deficient mutants. Specifically, we investigated binding of dofetilide to S631A-hERG and S620T-hERG. S631A-hERG has a markedly right-shifted $V_{0.5}$ of steady-state inactivation compared with WT-hERG that is very similar to that observed for N588K (Fig. 7A), whereas S620T-hERG does not inactivate at measurable voltages (Ficker et al., 1998). Therefore, at +20 mV, the proportion of channels in the open/inactivated states is ~85:15 for N588K and S631A, compared with 100:0 for S620T but 2:98 for WT-hERG (Fig. 7A).

The affinity of dofetilide for S631A-hERG was not statistically different from that for N588K-hERG [404 ± 95 nM (n = 4) and 377 ± 69 nM (n = 4), respectively], an 8-fold reduction compared with WT-hERG. That these two mutants, with very similar effects on inactivation but apparently not located near each other, have very similar effects on drug binding suggests that the reduced affinity for drug binding is mediated by reduced inactivation of the channel. However, the affinity of dofetilide for S620T was reduced a further 10-fold (3494 ± 374 nM, n = 4) (Fig. 7B) compared with its affinity for S631A or N588K. Given that there is relatively little difference in the extent to which S631A and N588K channels occupy the open state at +20 mV (the voltage at which we assayed drug binding) compared with S620T channels (i.e., ~85% compared with 100%), a marked reduction in drug affinity for S620T-hERG suggests a gating-independent effect on drug binding by this mutant. An alternative hypothesis is that despite the relative infrequency with which S631A and N588K channels occupy the inactivated state at +20 mV, the kinetics of drug binding and unbinding are such that whenever the channel enters the inactivated state, it binds drug that, with a very slow off-rate, remains bound for a long period. According to this hypothesis, binding of drug to the S620T mutant would only encounter the open state and so reflect the affinity for the open state, whereas binding to WT or N588K channels would reflect a weighted average of the affinity for the inactivated and open states dependent on the relative rates of transitions between the two states and drug binding and unbinding rates. To test this hypothesis, we set up a computer model of drug binding to hERG channels as depicted in Fig. 8.

Modeling Kinetics of Drug Binding to Open and Inactivated States. The Markov chain model for hERG kinetics is based on that developed by Lu et al. (2001) with the addition of two states: drug-bound open state, and drug-bound inactivated state (Fig. 8). The rate constants, scaled to 22°C, for the model are tabulated in the data supplement. To model the S620T mutant, the rate constants for transition steps to the inactivated state were set to 0. To model the N588K mutant, the rate constants for the transition between the open and inactivated states were adjusted to reproduce the experimentally observed changes in these rate constants and the steady-state inactivation (see data supplement). For simplicity, we assumed that the kinetics of activation were the same for WT-, S620T- and N588K-hERG channels.

To calculate the rate constants for open and inactivated drug-blocked state, we assumed that drug affinity for S620T represented the affinity for the open state. The rate constants for open-state drug block, *kf6* and *kb6*, were constrained to fit

TABLE 1
Collated IC_{50} values calculated from the Hill plots in Figs. 4 and 6
All IC_{50} values shown are mean ± S.E.M. (n cells). IC_{50} values for the eight drugs against N588-hERG, WT-hERG, and N588K-hERG.

	N588E	WT-hERG	N588K
Astemizole	4.8 ± 1.2 nM (5) n_H = 1.2	5.1 ± 1.4 nM (6) n_H = 1.0	14.8 ± 1.1 nM (5)* n_H = 0.8
Cisapride	13.9 ± 4.9 nM (4) n_H = 0.8	20.5 ± 2.2 nM (6) n_H = 1.0	55.9 ± 4.2 nM (6)* n_H = 0.9
Dofetilide	39.4 ± 7.3 nM (5) n_H = 1.1	51.0 ± 1.3 nM (9) n_H = 1.3	377.3 ± 57.8 nM (5)* n_H = 1.3
Terfenadine	48.2 ± 10.6 nM (5) n_H = 1.0	61.4 ± 16.2 nM (9) n_H = 1.2	170.2 ± 32.3 nM (7)* n_H = 0.9
Quinidine	3.71 ± 0.4 μM (4) n_H = 1.1	3.2 ± 0.3 μM (5) n_H = 0.8	3.9 ± 0.3 μM (4) n_H = 0.9
Perhexiline	5.0 ± 1.8 μM (5) n_H = 0.8	5.9 ± 0.9 μM (7) n_H = 1.1	4.7 ± 1.7 μM (5) n_H = 1.2
Erythromycin	98.4 ± 39.7 μM (5) n_H = 0.8	129.5 ± 59.9 μM (4) n_H = 0.7	151.1 ± 49.4 μM (4) n_H = 0.8
dl-Sotalol	585.6 ± 178.6 μM (4) n_H = 0.8	515.5 ± 35.5 μM (4) n_H = 0.9	1392.0 ± 266.5 μM (4)* n_H = 0.9

n_H, Hill coefficient calculated from the curve of best fit to the data (see Figs. 4 and 6).
* Significant difference from N588K to N588E and between N588K and WT-hERG.

the data for drug binding to the S620T channels. The values for *kf6* and *kb6* were then held constant, and the values for drug binding to the inactivated state, *kf7* and *kb7*, were constrained to fit the time course of drug block for WT channels. In the case of dofetilide binding, the calculated affinity for the open state (*kf6*/*kb6*) was 3.5 μM (i.e., the value for S620T), and the calculated affinity for the inactivated state (*kf7*/*kb7*) was 47.8 nM. The measured affinity for dofetilide binding to WT channels, 50.1 nM, is much closer to the calculated value for the affinity to the inactivated state reflecting both the greater proportion of time WT channels spend in the inactivated state and the slower dissociation of drug from the inactivated state. If the original assumption was correct (i.e., drug affinity for S620T is the true affinity of the drug for the open state), then substitution of the values for *kf6*, *kb6*, *kf7,* and *kb7* into our model for N588K should reproduce the experimentally determined IC_{50} value for dofetilide binding to N588K. As can be seen from the data in Fig. 9, the model-predicted values are very close to the experimental data. The same procedure was repeated for each of the state-dependent drugs formerly assessed (Fig. 10, A–D; Table 2) with similarly good approximations to the experimental data.

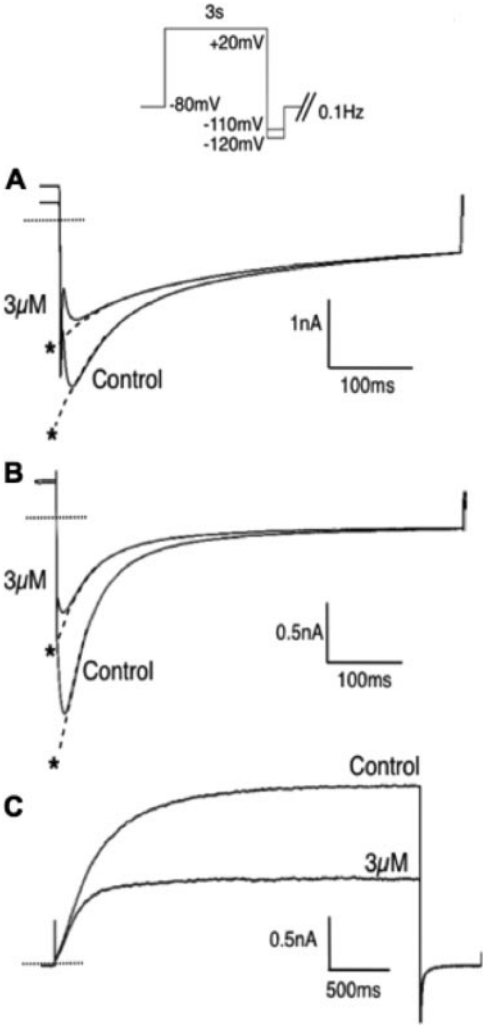

Fig. 5. Typical examples of current traces recorded from WT-hERG (A), N588E-hERG (B), and N588K-hERG (C) in the presence and absence of 3 μM quinidine. The drug block voltage protocol is shown at the top. Broken lines represent zero current in each case. Note the >50% of block of N588K-hERG by 3 μM quinidine, which is similar to the percentage block in WT-hERG and N588E-hERG. Rates of deactivation in N588E-hERG are faster than WT-hERG due to the use of a −120-mV "revelatory" voltage step to produce adequate opening of channels to measure current. The rate of deactivation seems to slow in A and B with application of drug; this is probably due to some drug unblocking during this step rather than to a true effect on the kinetics of deactivation.

Discussion

State Dependence of Drug Binding. Most drugs that block hERG require channel opening (Kiehn et al., 1996). Some evidence suggests that, once activated, inactivation increases drug affinity for the channel: first, mutant hERG channels with disrupted inactivation (S631A, S620T, and G628C/S631C) reduce drug block by multiple agents (Ficker et al., 1998; Lees-Miller et al., 2000; Numaguchi et al., 2000; Yang et al., 2004); and second, mutations introduced into bovine EAG and hEAG1 that enable inactivation also confer sensitivity to dofetilide block (Ficker et al., 2001, Gomez-Varela et al., 2006). However, the inactivation-disrupting mutations could affect drug block through gating-independent means. Ser631 and Ser620 lie proximate to the drug binding space, and mutations at these positions may produce conformational changes at the base of the pore helix, an important molecular determinant of drug binding (Mitcheson et al., 2000). G628C/S631C markedly reduces the potassium selectivity of hERG (Smith et al., 1996), suggesting a conformational change in the vicinity of the selectivity filter. Furthermore, mutant hERG channels G648A and T623A promote inactivation but reduce methane sulfonamide block of hERG (Mitcheson et al., 2000). In addition, voltage protocols designed to favor occupancy of the inactivated state during drug binding (i.e., large depolarizations) also relieve drug block (Kiehn et al., 1996; Numaguchi et al., 2000).

The data reported in this study provide strong evidence that drug binding to hERG K^+ channels is influenced by whether the channels are in the inactivated or the open state. In addition, we have demonstrated that this phenomenon is drug-dependent, with the ratio of affinities for the open to inactivated state varying from 1:1 (i.e., not state-dependent: quinidine, erythromycin, and perhexiline) to 1:70 (dofetilide). First, we have shown that a mutation, N588K, introduced into a region believed to be remote from the drug binding pocket (Yi et al., 2007) that shifts the voltage dependence of inactivation (Brugada et al., 2004; Clarke et al., 2006) affects drug binding. A combination of structural studies (Torres et al., 2003), toxin binding studies (Pardo-Lopez et al., 2002), and molecular dynamics modeling studies (Yi et al., 2007) suggests that Asn588 on the hydrophilic surface of the S5P α-helix faces the extracellular space and is therefore remote from the drug-binding pocket. Second, we have shown that two distinct mutants that have very similar effects on inactivation (N588K and S631A) have similar effects on drug binding. The simplest explanation is that it is the effect these

TABLE 2
Drug affinity for S620T (IC_{50})

Astemizole	19.8 ± 3.7 nM (n = 10)
Cisapride	157.1 ± 20.2 nM (n = 6)
Dofetilide	3494.4 ± 425.0 nM (n = 4)
dl-Sotalol	2218.2 ± 380.2 μM (n = 5)
Terfenadine	271.8 ± 120.3 nM (n = 4)

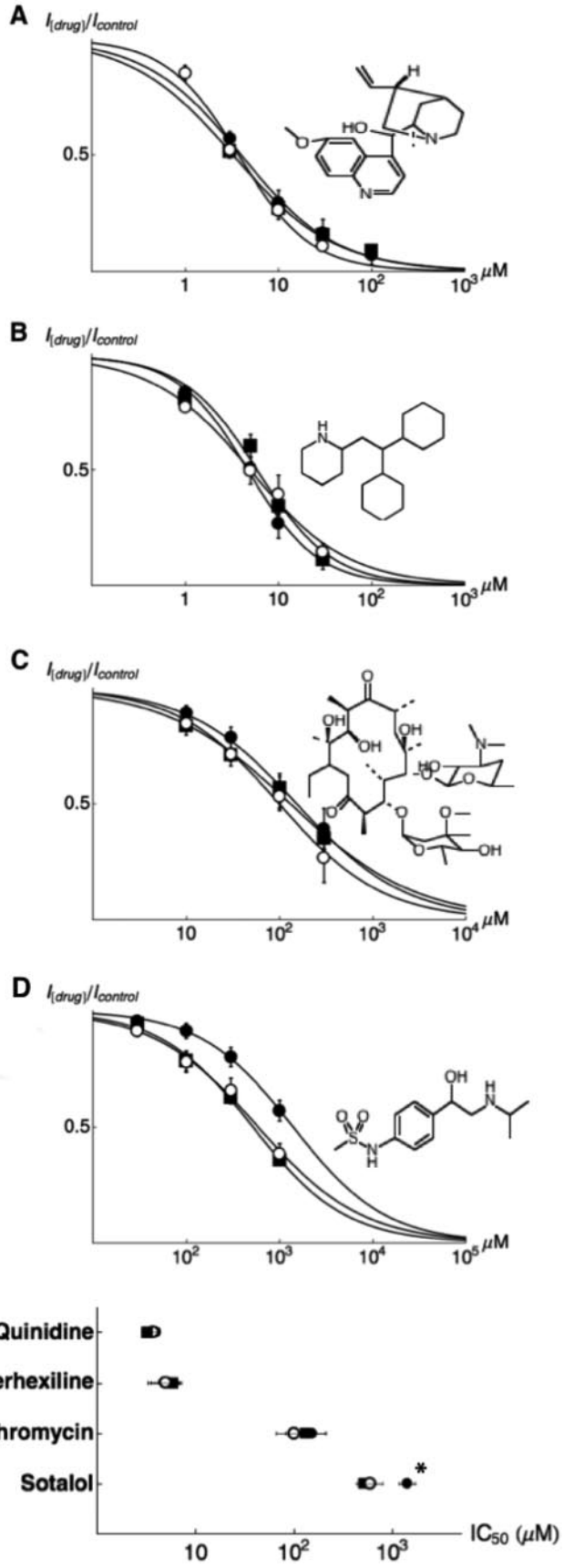

Fig. 6. Hill plots of low-affinity hERG blockers. Drug binding to WT-hERG (■), N588E-hERG (○), and N588K-hERG (●) for quinidine (A) perhexiline (B), erythromycin (C), and *dl*-sotalol (D). Each data point represents $I_{[drug]}/I_{control}$ ± S.E.M. for $n = 4$ to 6. E, summary data showing the mean IC_{50} ± S.E.M. for each drug. Significant differences between WT-hERG and N588K-hERG are denoted by ∗. All values are listed in Table 1.

mutations have on inactivation that accounts for the altered drug binding. Third, our kinetic modeling of drug binding to WT, S620T, and N588K mutant channels demonstrates that all of the differences in drug-binding between these mutants can be explained on the basis of differences in occupancy of open and inactivated states and the kinetics of drug binding. Our kinetic modeling studies have also enabled, for the first time, an estimation of the binding affinities for both the open and inactivated states for a range of drugs.

Stork et al. (2007) have recently published data extending the concept of state dependence to the dissociation of drugs from the hERG channel. As they have elegantly shown, some drugs require opening of the activation gate to dissociate from the inner cavity of the channel. Our data are complementary to their own, demonstrating that the rate of drug dissociation will depend not only on the relative proportions of activated and closed channels at a given voltage, but also

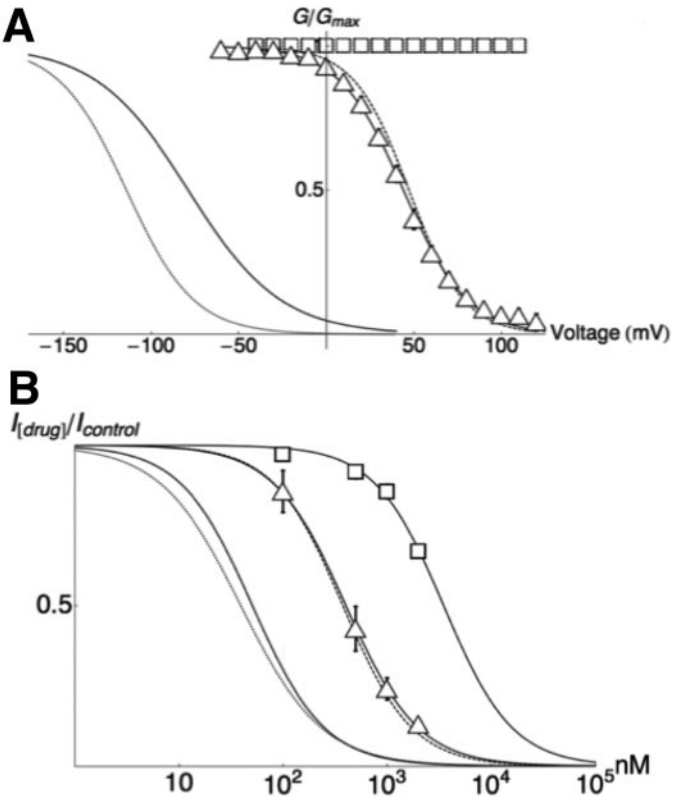

Fig. 7. A, conductance voltage curves for S631A-hERG (△) and S620T-hERG (□). Data points are mean ± S.E.M., and the curve fitted to the data points is a Boltzmann function. The $V_{0.5}$ value of steady-state inactivation for the S631A-hERG mutant is 43 ± 2 mV with a slope factor of −16.5 mV ($n = 6$). S620T-hERG does not inactivate in the voltage range shown (Ficker et al., 1998). Dotted, solid, and broken lines show data for N588E-hERG, WT-hERG, and N588K-hERG, reproduced from Fig. 2. B, the affinity of dofetilide for S631A-hERG (△) and S620T-hERG (□). Dotted, solid, and broken lines show data for N588E-hERG, WT-hERG, and N588K-hERG, respectively, reproduced from Fig. 4C. Note the similar drug affinity for the N588K and S631A cell constructs and the marked rightward shift (reduced affinity) of dofetilide for the S620T construct.

the proportion of activated channels in the inactivated or open state, itself a function of voltage.

In contrast with our data, there is one report in the literature that suggests mutations to Ser620 could have a gating-independent effect on drug binding (Guo et al., 2006). Guo and colleagues showed that S620T and S620C both abolished inactivation gating but had different affinities for E-4031, a methane sulfonamide similar to dofetilide. These data, however, are not necessarily incompatible with our results. It is possible that the abolition of inactivation alters drug affinity in both S620T and S620C. However, whereas the S620T represents the true affinity for the open state, the cysteine side chain in S620C is able to bind to the drug and thereby increase the affinity relative to that for S620T.

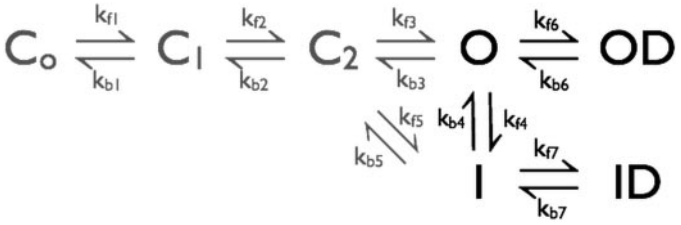

Fig. 8. Markov model of drug binding to hERG. C_x, closed states; O, open state; I, inactivated state; OD, drug bound to open state; ID, drug bound to inactivated state. Greyed out portions of the model were not altered during modeling simulations.

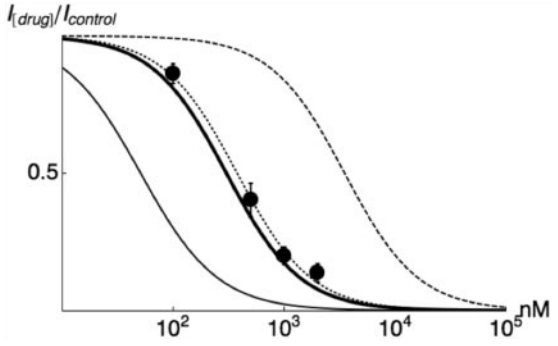

Fig. 9. Dofetilide Hill curves with data points for N588K-hERG and the modeling curve superimposed. Thin solid line, dotted line, and broken line show WT-, N588K-, and S620T-hERG, respectively. The modeled line is thick black. Experimental IC_{50} values for dofetilide block of N588K and the modeled values are 377 ± 57.8 and 302 nM, respectively.

What Explains the Strong Preference for Inactivated State Binding? The molecular determinants of drug binding to hERG include two aromatic residues in the Ser6 helix, Phe656 and Tyr652, and to a variable extent three residues close to the selectivity filter, Thr623, Ser624, Val625, and two residues in Ser6, Gly648 and Val659 (Fig. 1). In the absence of a high-resolution structure of hERG, the exact conformation of these residues in relation to each other cannot be determined. It has been suggested that inactivation of hERG channels involves changes in the structure of the pore region (Chen et al., 2002), and so the spatial relationships of the different components of the drug binding pocket are likely to vary between the open and inactivated state. One can imagine two scenarios that could arise. First, a conformational change around the selectivity filter and base of the pore-helix caused by inactivation (as has been suggested to occur in hERG) (Gang and Zhang, 2006) could result in a reorientation of the drug binding residues at the base of the selectivity filter relative to the drug binding residues on Ser6.

Second, inactivation could involve reorientation of the Ser6 helixes, relative to their positions in the open state. In this hypothesis, not only would the relationship between the drug binding residues on Ser6, Tyr652, and Phe656 alter with respect to drug binding residues at the base of the pore helixes (Lees-Miller et al., 2000; Chen et al., 2002) but also the intersubunit relationships between Tyr652 and Phe656 would change (Myokai et al., 2008). Evidence in favor of a primary role for reorientation of Ser6 in favoring inactivated state drug binding comes from a study investigating the effect of mutating Phe656 to methionine on the binding of droperidol (Luo et al., 2008). The affinity of droperidol for S631A-hERG was reduced compared with WT-hERG, but introduction of S631A into the background of the F656M mutant did not reduce the affinity compared with F656M-hERG alone.

The reduction in affinity of dofetilide for S620T-hERG com-

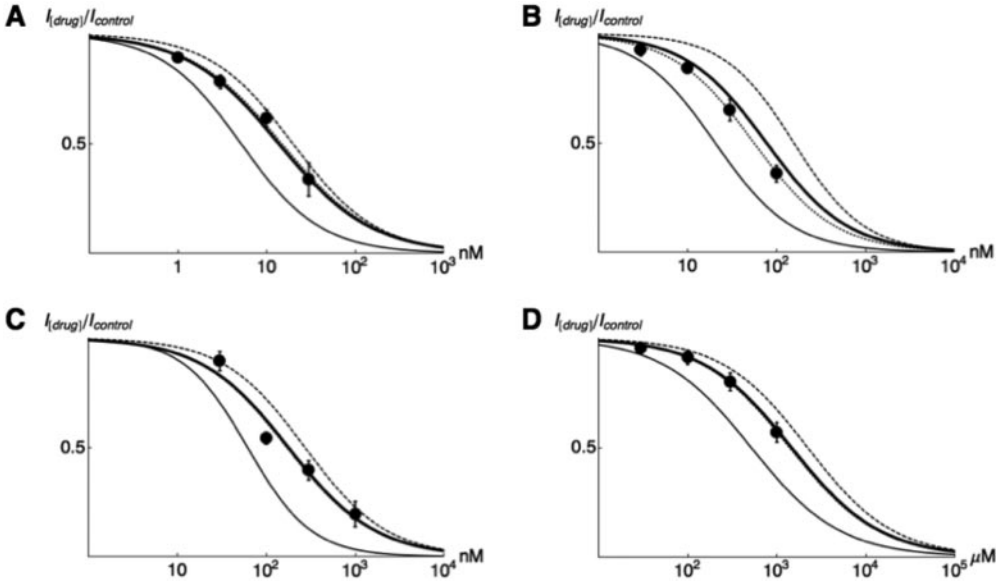

Fig. 10. Hill curves for astemizole (A), cisapride (B), terfenadine (C), and *dl*-sotalol (D) with data points for N588K-hERG and the modeling curves superimposed. Thin solid line, dotted line, and broken line show WT-, N588K-, and S620T-hERG, respectively. Modeled curves are thick black. Experimental IC_{50} values for drug block of N588K and the modeled values are the following, respectively: astemizole, 14.8 ± 1.1 versus 13.6 nM; cisapride, 55.9 ± 4.2 versus 77.3 nM; terfenadine, 170 ± 32.3 versus 177 nM; and *dl*-sotalol, 1392 ± 266.5 versus 1461 μM. Drug IC_{50} values for S620T-hERG are presented in Table 2; Hill plots for S620T-hERG are presented in the data supplement.

pared with WT-hERG (70-fold) is comparable with the reduction in drug affinities seen when residues Tyr652 or Phe656 are mutated (Lees-Miller et al., 2000; Mitcheson et al., 2000). This suggests that abolition of inactivation results in the complete elimination of one of the interactions between dofetilide and the channel. However, for astemizole, cisapride, sotalol, and terfenadine, the reduction in affinity is more modest, suggesting that an interaction has been reduced but not eliminated.

Inactivated State Binding Is Necessary but Not Sufficient for High-Affinity Binding. All of the high-affinity blockers tested in this study showed a marked preference for the inactivated state. At depolarized potentials, WT-hERG channels predominantly reside in the inactivated state; therefore, it is unsurprising that the drugs with the highest affinity for the inactivated state show the highest affinity for WT-hERG. However, our data for *dl*-sotalol clearly indicate that state dependence of binding is not sufficient to produce high-affinity binding. One plausible explanation for the low-affinity yet state dependence of *dl*-sotalol binding is that it binds to the residues most critical for state-dependent binding but does not bind to any other residues, whereas the higher-affinity state-dependent blockers bind both to the critical state-dependent residues and to others. If this hypothesis is correct, then determining the molecular basis of sotalol binding to hERG would be a useful probe for determining the minimum requirements for state-dependent binding to hERG.

Relevance for Drug-Binding in SQTS. The most common form of SQTS results from the N588K mutation in hERG (Brugada et al., 2004). The wide spectrum of drugs known to block hERG provides multiple candidates for treatment. However, initial testing demonstrated that *dl*-sotalol failed to prolong the QT interval (Brugada et al., 2004). Of the tested candidates, only quinidine (Gaita et al., 2004), disopyramide (McPate et al., 2006), and doxepin (Duncan et al., 2007) have been shown to block N588K at affinities similar to WT. It is significant that all block hERG in the micromolar (low-affinity) range. It is noteworthy that although the binding affinity of astemizole for N588K is reduced compared with WT, its affinity for N588K is 250-fold greater than quinidine. Combined with a benign side effect profile, it is a good candidate for evaluation as a treatment for SQTS type 1.

Relevance for High-Throughput Assays. Given the mandated need to screen all drugs for hERG binding, there has been considerable effort put into developing high-throughput screens for assaying drug binding to hERG (Tang et al., 2001; Dorn et al., 2005). In general, however, the results of these screens have been poor, and we suggest that this may be because they predominantly assay binding to the open state and therefore underestimate the affinity of drugs that preferentially bind the inactivated state. Given that the difference in affinity between the open and inactivated states can be 70-fold, it is important that any high-throughput screening system must assay binding to the inactivated state.

Conclusions

We investigated the relationship between inactivation gating and drug block of hERG, finding that high-affinity block (nanomolar range) is promoted by inactivation. The use of charged mutants at Asn588 provides a methodology for investigating the conformational changes of the channel pore between open and inactivated states. Furthermore, we have calculated for the first time the relative affinities of drug binding to the open and inactivated states of the hERG channel, which in the case of dofetilide shows a 70-fold greater affinity for the inactivated state. The pharmaceutical importance of these data is highlighted by the observation that two drugs (astemizole and terfenadine) that have been withdrawn from the market and one (cisapride) that has had its use severely restricted exhibit a marked preference for binding to the inactivated state. In this study, we have also identified astemizole as a high-affinity blocker of the mutant N588K-hERG channel and propose it as a possible therapeutic candidate for treatment of the life-threatening SQTS 1.

Acknowledgments

We thank Jane Bursill, Adam Hill, Stefan Mann, Tadeusz Marciniec, and Ken Wyse for excellent technical assistance and Catherine Clarke, Mark Hunter, and JingTing Zhao for useful discussions.

References

Brugada R, Hong K, Dumaine R, Cordeiro J, Gaita F, Borggrefe M, Menendez TM, Brugada J, Pollevick GD, Wolpert C, Burashnikov E, Matsuo K, Wu YS, Guerchicoff A, Bianchi F, Giustetto C, Schimpf R, Brugada P, and Antzelevitch C (2004) Sudden death associated with short-QT syndrome linked to mutations in HERG. *Circulation* **109:**30–35.

Cavalli A, Poluzzi E, De Ponti F, and Recanatini M (2002) Toward a pharmacophore for drugs inducing the long QT syndrome: insights from a CoMFA study of HERG K^+ channel blockers. *J Med Chem* **45:**3844–3853.

Chen J, Seebohm G, and Sanguinetti MC (2002) Position of aromatic residues in the S6 domain, not inactivation, dictates cisapride sensitivity of HERG and EAG potassium channels. *Proc Natl Acad Sci U S A* **99:**12461–12466.

Clarke CE, Hill AP, Zhao J, Kondo M, Subbiah RN, Campbell TJ, and Vandenberg JI (2006) Effect of S5P alpha-helix charge mutants on inactivation of hERG K+ channels. *J Physiol* **573:**291–304.

Cordeiro JM, Brugada R, Wu YS, Hong K, and Dumaine R (2005) Modulation of I_{Kr} inactivation by mutation N588K in KCNH2: a link to arrhythmogenesis in short QT syndrome. *Cardiovasc Res* **67:**498–509.

Curran ME, Splawski I, Timothy KW, Vincent GM, Green ED, and Keating MT (1995) A molecular basis for cardiac arrhythmia: HERG mutations cause long QT syndrome. *Cell* **80:**795–803.

Dorn A, Hermann F, Ebneth A, Bothmann H, Trube G, Christensen K, and Apfel C (2005) Evaluation of a high-throughput fluorescence assay method for HERG potassium channel inhibition. *J Biomol Screen* **10:**339–347.

Duncan RS, McPate MJ, Ridley JM, Gao Z, James AF, Leishman DJ, Leaney JL, Witchel HJ, and Hancox JC (2007) Inhibition of the HERG potassium channel by the tricyclic antidepressant doxepin. *Biochem Pharmacol* **74:**425–437.

Ficker E, Jarolimek W, and Brown AM (2001) Molecular determinants of inactivation and dofetilide block in ether a-go-go (EAG) channels and EAG-related K^+ channels. *Mol Pharmacol* **60:**1343–1348.

Ficker E, Jarolimek W, Kiehn J, Baumann A, and Brown AM (1998) Molecular determinants of dofetilide block of HERG K+ channels. *Circ Res* **82:**386–395.

Gaita F, Giustetto C, Bianchi F, Schimpf R, Haissaguerre M, Calò L, Brugada R, Antzelevitch C, Borggrefe M, and Wolpert C (2004) Short QT syndrome: pharmacological treatment. *J Am Coll Cardiol* **43:**1494–1499.

Gang H and Zhang S (2006) Na^+ permeation and block of hERG potassium channels. *J Gen Physiol* **128:**55–71.

Gómez-Varela D, Contreras-Jurado C, Furini S, García-Ferreiro R, Stühmer W, and Pardo LA (2006) Different relevance of inactivation and F468 residue in the mechanisms of hEag1 channel blockage by astemizole, imipramine and dofetilide. *FEBS Lett* **580:**5059–5066.

Guo J, Gang H, and Zhang S (2006) Molecular determinants of cocaine block of human ether-a-go-go-related gene potassium channels. *J Pharmacol Exp Ther* **317:**865–874.

Guth BD (2007) Preclinical cardiovascular risk assessment in modern drug development. *Toxicol Sci* **97:**4–20.

Kiehn J, Lacerda AE, Wible B, and Brown AM (1996) Molecular physiology and pharmacology of HERG. Single-channel currents and block by dofetilide. *Circulation* **94:**2572–2579.

Kirsch GE, Trepakova ES, Brimecombe JC, Sidach SS, Erickson HD, Kochan MC, Shyjka LM, Lacerda AE, and Brown AM (2004) Variability in the measurement of hERG potassium channel inhibition: effects of temperature and stimulus pattern. *J Pharmacol Toxicol Methods* **50:**93–101.

Lees-Miller JP, Duan Y, Teng GQ, and Duff HJ (2000) Molecular determinant of high-affinity dofetilide binding to HERG1 expressed in *Xenopus* oocytes: involvement of S6 sites. *Mol Pharmacol* **57:**367–374.

Lu Y, Mahaut-Smith MP, Varghese A, Huang CL, Kemp PR, and Vandenberg JI

(2001) Effects of premature stimulation on HERG K^+ channels. *J Physiol* **537:** 843–851.
Luo T, Luo A, Liu M, and Liu X (2008) Inhibition of the HERG channel by droperidol depends on channel gating and involves the S6 residue F656. *Anesth Analg* **106:**1161–1170.
McPate MJ, Duncan RS, Witchel HJ, and Hancox JC (2006) Disopyramide is an effective inhibitor of mutant HERG K+ channels involved in variant 1 short QT syndrome. *J Mol Cell Cardiol* **41:**563–566.
Mitcheson JS (2008) hERG potassium channels and the structural basis of drug-induced arrhythmias. *Chem Res Toxicol* **21:**1005–1010.
Mitcheson JS, Chen J, Lin M, Culberson C, and Sanguinetti MC (2000) A structural basis for drug-induced long QT syndrome. *Proc Natl Acad Sci U S A* **97:**12329–12333.
Mohammad S, Zhou Z, Gong Q, and January CT (1997) Blockage of the HERG human cardiac K^+ channel by the gastrointestinal prokinetic agent cisapride. *Am J Physiol* **273:**H2534–H2538.
Myokai T, Ryu S, Shimizu H, and Oiki S (2008) Topological mapping of the asymmetric drug-binding to the HERG potassium channel by use of tandem dimers. *Mol Pharmacol* **73:**1643–1651.
Numaguchi H, Mullins FM, Johnson JP Jr, Johns DC, Po SS, Yang IC, Tomaselli GF, and Balser JR (2000) Probing the interaction between inactivation gating and Dd-sotalol block of HERG. *Circ Res* **87:**1012–1018.
Pardo-Lopez L, Zhang M, Liu J, Jiang M, Possani LD, and Tseng GN (2002) Mapping the binding site of a human ether-a-go-go-related gene-specific peptide toxin (ErgTx) to the channel's outer vestibule. *J Biol Chem* **277:**16403–16411.
Roden DM (2004) Drug-induced prolongation of the QT interval. *N Engl J Med* **350:**1013–1022.
Roden DM (2008) Clinical practice. Long-QT syndrome. *N Engl J Med* **358:**169–176.
Sanguinetti MC, Jiang C, Curran ME, and Keating MT (1995) A mechanistic link between an inherited and an acquired cardiac arrhythmia: HERG encodes the IKr potassium channel. *Cell* **81:**299–307.
Smith PL, Baukrowitz T, and Yellen G (1996) The inward rectification mechanism of the HERG cardiac potassium channel. *Nature* **379:**833–836.
Stork D, Timin EN, Berjukow S, Huber C, Hohaus A, Auer M, and Hering S (2007) State dependent dissociation of HERG channel inhibitors. *Br J Pharmacol* **151:** 1368–1376.
Tang W, Kang J, Wu X, Rampe D, Wang L, Shen H, Li Z, Dunnington D, and Garyantes T (2001) Development and evaluation of high throughput functional assay methods for HERG potassium channel. *J Biomol Screen* **6:**325–331.
Torres AM, Bansal PS, Sunde M, Clarke CE, Bursill JA, Smith DJ, Bauskin A, Breit SN, Campbell TJ, Alewood PF, et al. (2003) Structure of the HERG K^+ channel S5P extracellular linker: role of an amphipathic α-helix in C-type inactivation. *J Biol Chem* **278:**42136–42148.
Volberg WA, Koci BJ, Su W, Lin J, and Zhou J (2002) Blockade of human cardiac potassium channel human ether-a-go-go-related gene (HERG) by macrolide antibiotics. *J Pharmacol Exp Ther* **302:**320–327.
Walker BD, Valenzuela SM, Singleton CB, Tie H, Bursill JA, Wyse KR, Qiu MR, Breit SN, and Campbell TJ (1999a) Inhibition of HERG channels stably expressed in a mammalian cell line by the antianginal agent perhexiline maleate. *Br J Pharmacol* **127:**243–251.
Walker BD, Singleton CB, Bursill JA, Wyse KR, Valenzuela SM, Qiu MR, Breit SN, and Campbell TJ (1999b) Inhibition of the human ether-a-go-go-related gene (HERG) potassium channel by cisapride: affinity for open and inactivated states. *Br J Pharmacol* **128:**444–450.
Weerapura M, Hébert TE, and Nattel S (2002) Dofetilide block involves interactions with open and inactivated states of HERG channels. *Pflugers Arch* **443:**520–531.
Yang BF, Xu DH, Xu CQ, Li Z, Du ZM, Wang HZ, and Dong DL (2004) Inactivation gating determines drug potency: a common mechanism for drug blockade of HERG channels. *Acta Pharmacol Sin* **25:**554–560.
Yi H, Cao Z, Yin S, Dai C, Wu Y, and Li W (2007) Interaction simulation of hERG K+ channel with its specific BeKm-1 peptide: insights into the selectivity of molecular recognition. *J Proteome Res* **6:**611–620.
Zhou Z, Vorperian VR, Gong Q, Zhang S, and January CT (1999) Block of HERG potassium channels by the antihistamine astemizole and its metabolites desmethylastemizole and norastemizole. *J Cardiovasc Electrophysiol* **10:**836–843.

Address correspondence to: Dr. Jamie I. Vandenberg, Victor Chang Cardiac Research Institute, 384 Victoria Street, Darlinghurst, NSW 2010, Australia. E-mail: j.vandenberg@victorchang.edu.au